

# Source versus differentiation controls on U-series disequilibria: Insights from Cotopaxi Volcano, Ecuador

Jennifer Garrison <sup>a,\*</sup>, Jon Davidson <sup>b</sup>, Mary Reid <sup>c</sup>, Simon Turner <sup>d</sup>

<sup>a</sup> Department of Geosciences, Univ. of Iowa, Iowa City, IA 52242, USA

<sup>b</sup> Department of Earth Sciences, Univ. of Durham, Durham, DH13LE, UK

<sup>c</sup> Department of Geology, Northern Arizona Univ. Flagstaff, AZ, 86011, USA

<sup>d</sup> Department of Earth and Planetary Sciences, Macquarie Univ. Sydney, NSW 2109, Australia

Received 18 August 2005; received in revised form 29 January 2006; accepted 6 February 2006

Available online 24 March 2006

Editor: K. Farley

## Abstract

Although the majority of young volcanic rocks in island arcs typically have <sup>238</sup>U excesses, continental arc rocks display both <sup>238</sup>U and <sup>230</sup>Th excesses. In fact, there is a global correlation between the sense of U-series disequilibria and crustal thickness that suggests that crustal thickness may somehow influence the processes that fractionate U from Th. At Cotopaxi Volcano, Ecuador, (<sup>238</sup>U)/(<sup>230</sup>Th) values of 1.03–1.14 in rhyolites are attributed to accessory phase fractionation, whereas (<sup>238</sup>U)/(<sup>230</sup>Th) values of 0.96–1.07 in andesites can be explained by several potential processes, including melting of garnet-bearing lower crust. The Cotopaxi rocks have non-fractionated HFSE ratios and La/Yb values that are consistent with melting of a garnet-bearing lithology, and we suggest a model of lower crustal melting and assimilation to account for the range of U-series data in the Cotopaxi andesites. Mantle like <sup>87</sup>Sr/<sup>86</sup>Sr and <sup>143</sup>Nd/<sup>144</sup>Nd values indicate that the assimilate was a relatively juvenile and/or mafic component. The rhyolites contain apatite and allanite, fractionation of which can generate <sup>238</sup>U excesses during crystallization, and modeling shows that 70–90% crystallization of an assemblage containing these phases could generate the observed <sup>238</sup>U excesses. These data suggest that multi-level AFC processes contribute to magma evolution at Cotopaxi Volcano as magma traverses the continental crust of the Northern Volcanic Zone. On the basis of the <sup>238</sup>U–<sup>230</sup>Th–<sup>226</sup>Ra data, the time for assimilation and ascent of the andesites was <8000 yr, whereas the rhyolites may have resided in the crust for 70–100ky. The modification of U–Th isotopic signatures may be a common feature of differentiated magmas in continental arc settings and such potential effects should be considered along with interpretations involving variable mantle sources and melting regimes.

© 2006 Elsevier B.V. All rights reserved.

**Keywords:** U-series; Ecuador; Cotopaxi; lower crustal melting; rhyolite

## 1. Introduction

The magnitude of disequilibrium in the <sup>238</sup>U decay chain provides a potent means of assessing the dynamics of magmatic processes, and as the compilation of global U-series data increases, general trends in <sup>238</sup>U and <sup>230</sup>Th disequilibria in specific tectonic settings have become more apparent. For example, whereas MORB and OIB

\* Corresponding author. Tel.: +1 319 335 1799; fax: +1 319 335 1821.

E-mail addresses: [jennifer-m-garrison@uiowa.edu](mailto:jennifer-m-garrison@uiowa.edu) (J. Garrison), [j.p.davidson@durham.ac.uk](mailto:j.p.davidson@durham.ac.uk) (J. Davidson), [Mary.Reid@NAU.EDU](mailto:Mary.Reid@NAU.EDU) (M. Reid), [sturner@els.mq.edu.au](mailto:sturner@els.mq.edu.au) (S. Turner).

are often characterized by  $^{230}\text{Th}$  excesses, volcanic arc rocks are often characterized by both  $^{238}\text{U}$  and  $^{230}\text{Th}$  excesses. The majority of young island arc rocks have  $^{238}\text{U}$  excesses that are typically attributed to addition of fluids from the subducting plate to the mantle wedge [1–8].  $^{238}\text{U}$  excesses of up to 45% ( $(^{238}\text{U})/(^{230}\text{Th})=1.45$ ) in island arc lavas indicate that transfer time of U from the slab into the mantle wedge and to the surface (U-

recycling) can be quite short, due in part to the thin oceanic crust (10–15 km) above most island arcs.

In continental arcs where the crust is thick (e.g., the Central Andes), it might be expected that magma ascent, storage and U-recycling times would be longer than in island arcs. This conjecture is supported by the abundance of calderas and highly evolved rocks that exist primarily in continental arcs. Longer recycling

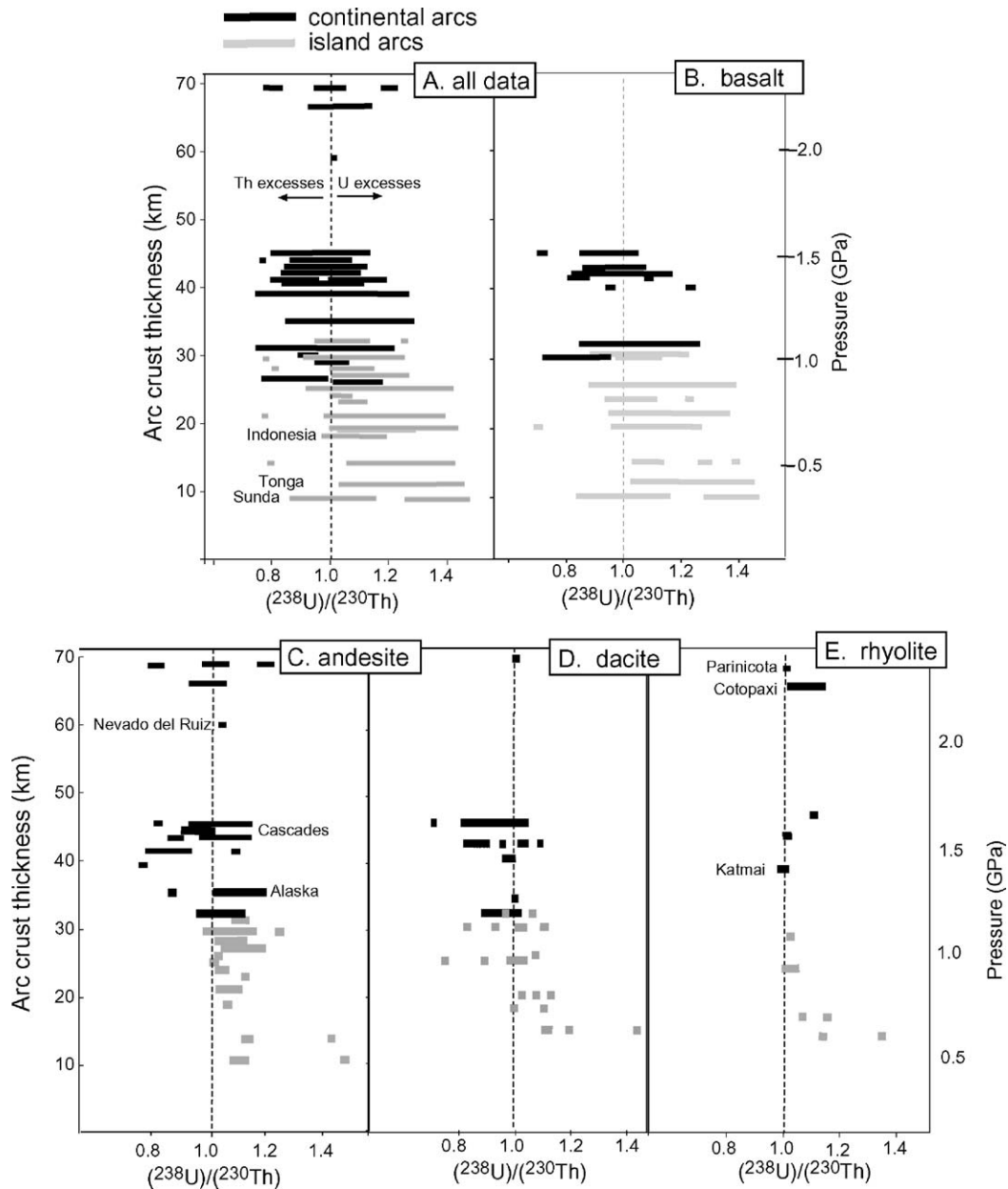


Fig. 1. (A) Compilation of global U–Th data, showing a correlation between  $(^{230}\text{Th})/(^{238}\text{U})$  and crustal thickness (km). Pressure is given in GPa. Data compiled from Turner et al. [2], and references therein. (B) The same data from part 1 (A), filtered to show only basalt, (C) andesite, (D) dacite and (E) rhyolite. The black solid lines represent continental arcs, and the gray lines represent island arcs.

times and continual ingrowth of  $^{230}\text{Th}$  would result in continental arc lavas being closer to equilibrium (i.e.,  $(^{238}\text{U}/^{230}\text{Th})=1.0$ ) than their island arc counterparts. Continental arc rocks should therefore be closer to equilibrium simply due to the effect of ageing, and crustal thickness should correlate inversely with magnitude of  $^{238}\text{U}$  excesses. Continental arc rocks, however, often have significant  $^{230}\text{Th}$  excesses [9–11]. In fact, an overview of global U-series data shows that, in the most general sense, the degree of  $^{230}\text{Th}$  excess is greatest in volcanic arcs where the crust is also thick (Fig. 1). This is not what would be predicted if ageing were the only process acting on source-derived U-series fractionation. Fig. 1 also illustrates that the maximum  $^{238}\text{U}$  excesses are not as great in continental arcs as they are in island arcs, and that basalts and andesites from island arcs primarily have  $^{238}\text{U}$  excesses (Fig. 1B,C), whereas continental arcs may have  $^{238}\text{U}$

excesses as well as  $^{230}\text{Th}$  excesses in a given volcano (Fig. 1C).

These observations suggest that crustal thickness may influence the degree of disequilibrium in basalts and andesites by dampening  $^{238}\text{U}$  excesses and generating  $^{230}\text{Th}$  excesses. This trend may reflect preferential retention of U in residual garnet or Al-rich clinopyroxene in the crust or mantle at pressures greater than 1.5 GPa where  $D_{\text{U}}/D_{\text{Th}} \gg 1$  for both minerals [12]. Residual garnet and pyroxene could produce significant U–Th fractionation in low degree partial melts, whereas mineral fractionation will only produce U–Th disequilibrium at relatively high degrees of crystallization (i.e., low melt fraction), particularly if  $D$  values are low. In rhyolite, U–Th fractionation could be caused by very small degrees of crystallization of accessory phases that have very high  $D$  values [13]. In this paper, we explore the potential causes of  $^{230}\text{Th}$  and  $^{238}\text{U}$  excesses in

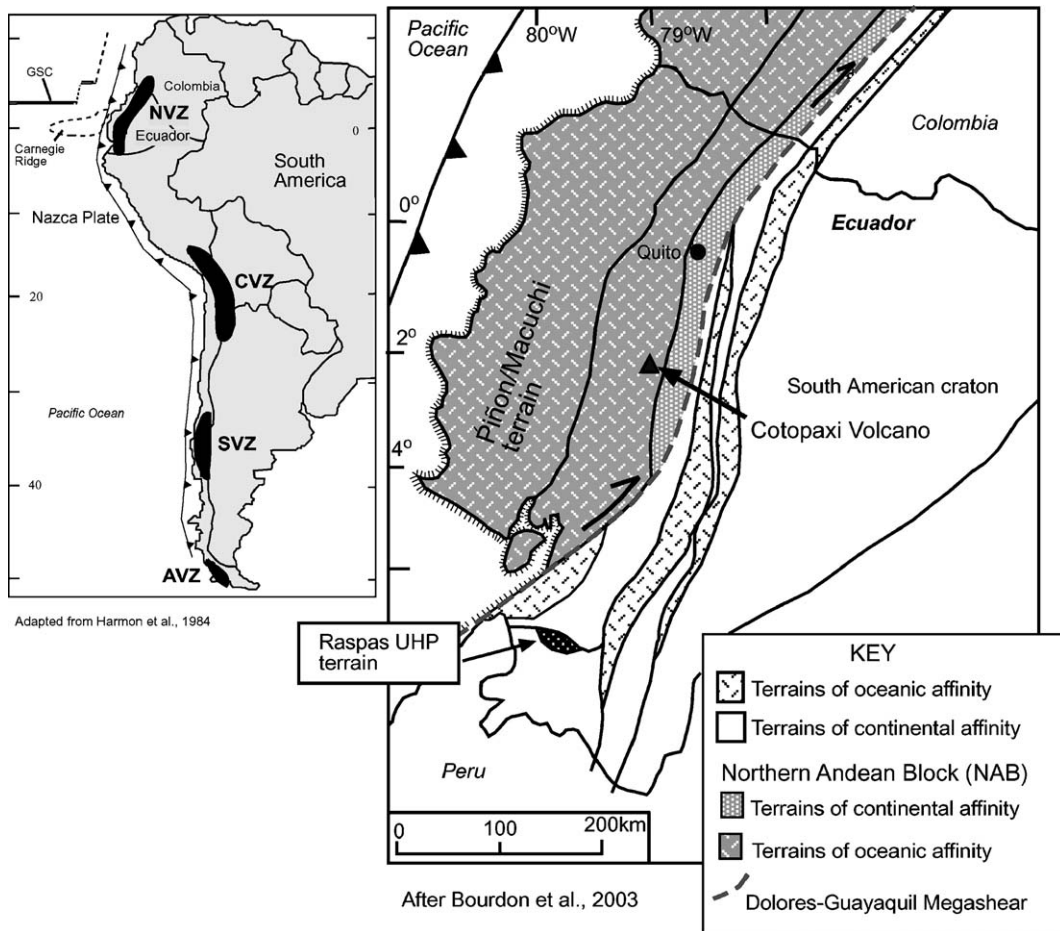


Fig. 2. Location map of S. America, showing the location of Cotopaxi Volcano in Ecuador and the Raspas UHP terrain in southern Ecuador. Also shown are the terrains of the Northern Andean Block, which is a block of oceanic accreted terrain (Pinon–Macuchi terrain). NVZ, CVZ, SVZ, AVZ=Northern, Central, Southern and Austral Volcanic Zones, respectively.

continental arc lavas, and present data from Cotopaxi Volcano, Ecuador to show that crustal processes can create variable  $^{238}\text{U}$  and  $^{230}\text{Th}$  excesses. This work also illustrates the complexities involved in interpreting U-series data in continental arc rocks. Cotopaxi Volcano is ideal for this study because 1) compositionally diverse magmas are represented, 2) both rhyolite and andesite have been modified by crustal interaction, and 3) the Cotopaxi rocks have excesses of  $^{230}\text{Th}$  and  $^{238}\text{U}$ .

## 2. Background

### 2.1. U-series systematics

Comprehensive introductions to U-series systematics are given by Bourdon et al. [14], and Ivanovich and Harmon [15].  $^{238}\text{U}$  decays in several steps to  $^{230}\text{Th}$ , which decays to  $^{226}\text{Ra}$ . Any geologic process that fractionates U, Th and/or Ra from each other causes radioactive disequilibrium in the system, and the system will then return to radioactive secular equilibrium through either net ingrowth or decay of  $^{230}\text{Th}$  and/or  $^{226}\text{Ra}$ . The return to equilibrium is time dependent and effectively takes place over approximately five half-lives of the daughter isotope. For  $^{230}\text{Th}$ , equilibrium is attained after approximately 350 ka, whereas for  $^{226}\text{Ra}$  equilibrium is attained after 8000 yr. This characteristic allows us to constrain the time since fractionation of the U, Th and Ra nuclides.

### 2.2. Cotopaxi Volcano and the Northern Volcanic Zone

Cotopaxi Volcano ( $1^{\circ}15'\text{S}$ ,  $78^{\circ}25'\text{W}$ ; 5800 m) is located in the Northern Volcanic Zone (NVZ) of the South American Andes, ~60 km southwest of the capital city of Quito in central Ecuador (Fig. 2). The NVZ is the northernmost zone of active volcanism in the Andean Cordillera, and extends from  $5^{\circ}\text{N}$ – $2^{\circ}\text{S}$ . Lava flows and pyroclastic fall deposits that are traceable to the Cotopaxi vent were erupted between 7.2 ka ago and 1877 AD, as recorded by  $^{14}\text{C}$  ages of soil and peat units. Cotopaxi has erupted only andesite since approximately 4.5 ka, whereas between 7.2 and 4.6 ka, andesite eruptions were punctuated by rhyolite events [16,17, also M. Hall and P. Mothes, pers. com.].

The basement geology of the NVZ is complicated by the presence of accreted mafic terrain (Pinon–Macuchi island arc) of the Northern Andean Block (NAB). A major tectonic boundary—the Dolores–Guayaquil megashear—separates this terrain from the rest of Ecuador [18]. Gravity data show that the crust of the NVZ ranges in average thickness from ~20 km near the

coast to approximately 70 km underneath the Andean Cordillera [18]. The sub-arc basement is believed to comprise eclogite facies rocks similar to those of the Raspas UHP complex that are exhumed in SW Ecuador (Fig. 2) [19,20]. This terrain is interpreted to be the metamorphosed equivalent of the Macuchi island arc terrain of western Ecuador.

## 3. Analytical methods

Samples collected from Cotopaxi Volcano were chosen for analyses to reflect the range of ages and compositions of pyroclastic deposits. Pyroclastic falls were used almost exclusively; lava flows were used only when eruption ages could be accurately determined. The benefit of using pyroclastic falls instead of lava flows is that pyroclastic falls are regional topography-blanketing deposits that form a more continuous and complete stratigraphy. Geochemical data from pyroclastic falls can be suspect due to the effects of alteration, however a series of leaching experiments showed the degree of alteration to be minimal, and not affecting the conclusions of this research [17].

Samples were analyzed for trace and major elements at the GeoAnalytical Lab in Pullman, Washington and for Sr and Nd isotopes at the Keck Geochemistry lab at UCLA. A subgroup of samples was chosen for mineral separates and analyzed for U–Th–Ra disequilibria, and Table Mountain Latite (TML) was run as a comparative rock standard. Minerals were separated using methylene iodide, and individual separates were then hand-picked to ensure the highest possible purity. The glass fractions were ground and put in heavy liquids to separate accessory minerals. The analytical techniques for the U–Th separation followed the methods described in George et al. [21], and the  $^{238}\text{U}$ – $^{230}\text{Th}$  measurements were performed using a ThermoFinnigan Neptune multi-collector ICP-MS at the University of Bristol, UK. A total of fifteen whole rocks (ten andesites and five rhyolites) were analyzed for  $^{238}\text{U}$ – $^{230}\text{Th}$  disequilibria, in addition to minerals and glass from two of the rhyolites and two of the andesites. Blanks were analyzed to monitor contamination. Four andesites with eruption ages between 128 and ~1000 yr old were subsequently analyzed for  $^{226}\text{Ra}$  concentrations that were then used to calculate  $^{226}\text{Ra}/^{230}\text{Th}$  disequilibria. Ra purification followed the methods described in Turner et al. [6] and the analyses were performed on a ThermoFinnigan Triton thermal mass spectrometer at the University of Bristol.

Seven zircon grains, each one at least 40–60 μm in diameter were separated from the most evolved

Cotopaxi rhyolite (CTX-17), mounted in epoxy with zircon standards AS-3 and 91-500, highly polished and Au-coated in preparation for  $^{238}\text{U}$ – $^{230}\text{Th}$  analyses using the Cameca IMS 1270 ion microprobe. Zoning patterns were imaged using a LEO 1430VP scanning electron microscope cathodoluminescence detector. Following the procedure outlined in Reid et al. [22], microprobe ion analyses were conducted using a 10 nA primary  $^{16}\text{O}$ -beam and a spot size of  $\sim 30\text{ nm}$ . The U/Th ratios were measured by calibrating with  $\text{UO}^+$  and  $\text{ThO}^+$ . The same grains were also analyzed for U–Pb ages using the method described in Dalrymple et al. [23]. U–Pb ages were corrected for initial U–Th disequilibrium using the method of Schaerer [24].

## 4. Results

### 4.1. Petrography

The most mafic andesites (56–57 wt.%  $\text{SiO}_2$ ) from Cotopaxi have glomerocrysts that contain intergrown orthopyroxene, clinopyroxene and plagioclase. Plagioclase and pyroxene also exist as individual grains, and several populations of plagioclase can be identified on

the basis of zoning and resorption patterns. For example, some plagioclase grains have highly resorbed cores and pristine rims, others have pristine cores and resorbed rims, and still others show pervasive resorption with no pristine cores or rims. Individual pyroxene grains are euhedral to subhedral and appear more pristine. These andesites contain “micro-enclaves” that are small blebs of microcrystalline material that may be co-magmatic or xenocrystic, and micro-xenoliths (0.5 mm diam.) of metamorphic rock. The higher  $\text{SiO}_2$  andesites ( $\text{SiO}_2 > 57\text{ wt.}\%$ ) also contain clinopyroxene, orthopyroxene and plagioclase, however the pyroxene crystals in these samples are very resorbed and altered, and none of the grains are present as glomerocrysts. Unlike the lower  $\text{SiO}_2$  andesites, the plagioclase grains in these rocks are euhedral–subhedral and do not have pervasive disequilibrium textures.

The Cotopaxi rhyolites are nearly aphyric and contain  $\sim 2\%$  crystals, including quartz, amphibole, plagioclase, biotite, Fe–Ti oxides, apatite, zircon and allanite (or possibly chevkinite). Plagioclase crystals are euhedral and normally zoned, with no obvious resorption. Amphibole crystals do not have reaction rims, and are present in only the least evolved rhyolite. Quartz is

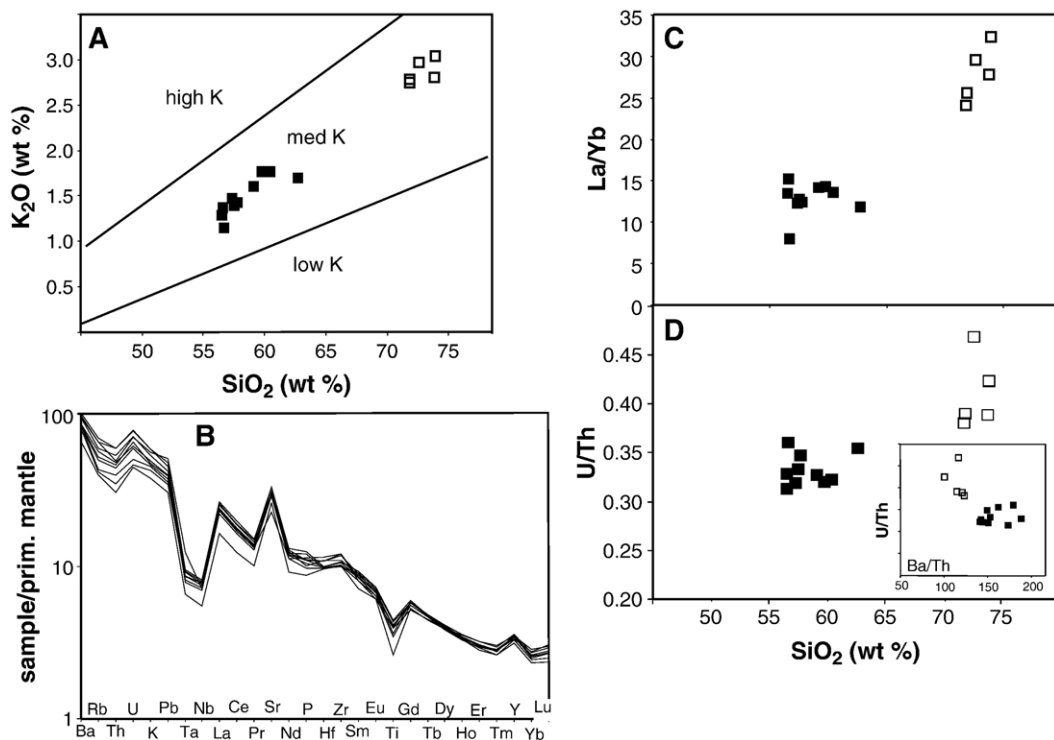


Fig. 3. (A)  $\text{K}_2\text{O}$  vs.  $\text{SiO}_2$  diagram for Cotopaxi andesites and rhyolites. Fields from Le Maitre et al. [74]. (B) Incompatible trace element diagram normalized to primitive mantle values of Sun and McDonough [75]. (C)  $\text{La/Yb}$  vs.  $\text{SiO}_2$  and (D)  $\text{U/Th}$  vs.  $\text{SiO}_2$  for the Cotopaxi andesites and the Cotopaxi rhyolites. Inset is  $\text{Ba/Th}$  vs.  $\text{U/Th}$ .  $\text{U/Th}$  scale is the same as in the main figure.

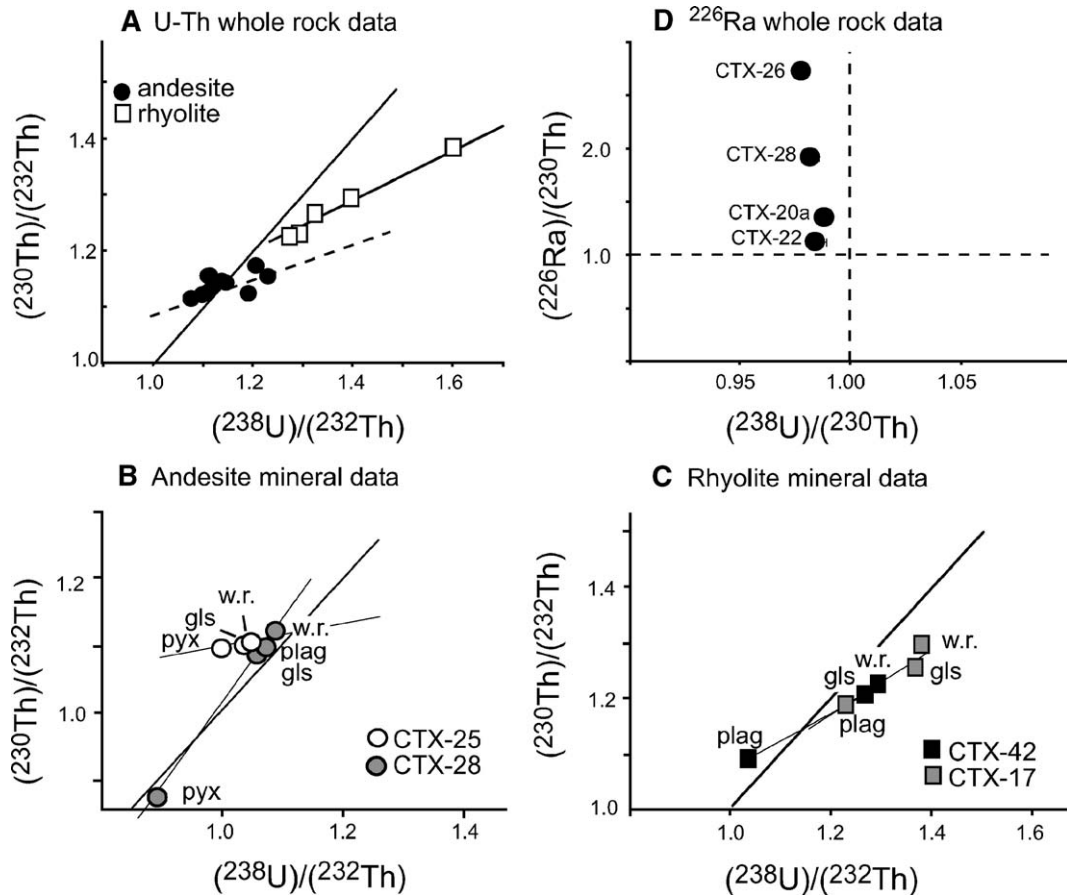


Fig. 4.  $(^{238}\text{U})/(^{230}\text{Th})$  equiline diagrams showing (A) the Cotopaxi rhyolite and andesite whole rock data, (B)  $(^{226}\text{Ra})/(^{230}\text{Th})$  data for four of the Cotopaxi andesites, (C) mineral separates from two Cotopaxi andesites, and (D) mineral separates for two Cotopaxi rhyolites ( $2\sigma$  error bars are smaller than the symbol size). Trend lines through the data represent isochrons calculated using the York regression method. The dashed isochron in (A) represents a linear trend that is not interpreted to signify an age.

present only in the most evolved rhyolite, and does not occur in conjunction with the amphibole. Apatite is present as small needles in all the rhyolites, and allanite (or chevkinite) crystals  $<100\mu\text{m}$  in length were found only in the most evolved rhyolite. Zircon grains are 30–70  $\mu\text{m}$  in diameter, and are subhedral or anhedral, rounded crystals.

#### 4.2. Geochemistry

In general, the medium- $\text{K}_2\text{O}$  andesites and rhyolites (Fig. 3A) from Cotopaxi have trace element characteristics that reflect their subduction zone origin (Fig. 3B). The full data set for Cotopaxi Volcano is presented in Garrison [17] and the data for this paper are reproduced as an electronic supplement (Table A.1.a, b) 1.<sup>1</sup> In

general, the Cotopaxi andesites are chemically similar to each other (Fig. 3B), however the rhyolites have elevated La/Yb and U/Th ratios (Fig. 3C, D). Andesite U/Th ratios do not vary systematically with trace element or major element concentrations, including ratios involving fluid mobile elements (i.e., Ba/Th) (inset, Fig. 3D).

#### 4.3. Th isotope disequilibria

##### 4.3.1. Whole rocks

Of the ten andesite whole rocks analyzed for U-series isotopes, seven have age-corrected equilibrium U–Th values or  $^{230}\text{Th}$  excesses of 1–4%, (Fig. 4A, Table 1a), and three have  $^{238}\text{U}$  excesses of 3–7%. These data form a linear array on an equiline (Th isochron) diagram. If taken as an isochron, this equates to an age of  $78.0^{+8.0}_{-7.5}$  ka (Fig. 4A). Absolute U and Th concentrations in the andesites vary by

<sup>1</sup> See Tables A.1.a and A.1.b in the online version of this paper.

Table 1a

U-series data for Cotopaxi: whole rocks

U–Th–Ra results for Cotopaxi whole rocks										
Sample	U (ug/g)	Th (ug/g)	<sup>226</sup> Ra (fg/g)	2σ	( <sup>230</sup> Th/ <sup>232</sup> Th)	2σ	( <sup>238</sup> U/ <sup>230</sup> Th)	2σ	<sup>234</sup> U/ <sup>238</sup> U	<sup>226</sup> Ra/ <sup>230</sup> Th
Andesite whole rocks										
CTX-20a	0.57	1.52	491	0.005	1.146	0.003	0.991	0.005	1.006	1.364
CTX-21	1.43	4.03		0.009	1.115	0.003	0.967	0.008	1.006	
CTX-22	1.83	5.00	715	0.007	1.125	0.002	0.986	0.006	1.004	1.128
CTX-25	1.84	5.02		0.014	1.155	0.002	0.963	0.012	1.004	
CTX-26	0.74	2.06	710	0.013	1.122	0.005	0.978	0.013	1.007	2.732
CTX-28	0.84	2.28	561	0.007	1.137	0.002	0.983	0.006	1.007	1.926
CTX-29	1.51	3.85		0.008	1.124	0.002	1.060	0.007	1.008	
CTX 34M	1.63	4.11		0.005	1.173	0.003	1.027	0.005	1.007	
CTX-61	1.01	2.49		0.016	1.154	0.004	1.067	0.014	1.004	
CTX-122	1.17	3.11		0.005	1.145	0.003	0.998	0.005	1.006	
TML <sup>a</sup>	10.00	29.00	992	0.007	1.068	0.001	1.013	0.006	1.005	1.009
Rhyolite whole rocks										
CTX-15	3.05	7.29		0.008	1.233	0.005	1.032	0.008	1.005	
CTX-17	3.67	7.99		0.009	1.295	0.006	1.076	0.009	1.008	
CTX-19	3.01	7.08		0.013	1.228	0.004	1.052	0.011	1.004	
CTX-42	3.21	7.51		0.009	1.262	0.002	1.026	0.007	1.002	
CTX-67	3.98	7.68		0.009	1.389	0.005	1.132	0.008	1.003	

All data are decay corrected.

<sup>a</sup> TML — Table Mountain Latite.

more than a factor of three. The four samples analyzed for <sup>226</sup>Ra–<sup>230</sup>Th disequilibria (CTX-22, CTX-26, CTX-20a and CTX-28) have (<sup>226</sup>Ra)/(<sup>230</sup>Th) from 1.13–2.73 (Fig. 4B, Table 1a) and <sup>230</sup>Th excesses of 1–2%. There is no correlation between the <sup>230</sup>Th and <sup>238</sup>U excesses and mineral percentages or eruption ages [17].

The five Cotopaxi rhyolites have <sup>238</sup>U excesses of 3–14% (Fig. 4A). In general, (<sup>230</sup>Th)/(<sup>232</sup>Th) of the rhyolites are more variable than those of the andesites. The absolute U and Th concentrations are also higher than those of the andesites. The rhyolite whole rock data taken together form a linear array that equates to an age of 74.1<sup>+5.5</sup><sub>-5.2</sub> ka (Fig. 4A).

Table 1b

U-series data for Cotopaxi: mineral separates

U–Th results for Cotopaxi mineral separates										
Sample	U (ppm)	Th (ppm)	( <sup>238</sup> U/ <sup>232</sup> Th)	2σ	( <sup>230</sup> Th/ <sup>232</sup> Th)	2σ	( <sup>238</sup> U/ <sup>230</sup> Th)	2σ	<sup>234</sup> U/ <sup>238</sup> Th	
CTX 25										
Whole rock	1.84	5.02	1.112	0.014	1.155	0.002	0.963	0.012	1.004	
Glass	1.61	4.41	1.106	0.008	1.154	0.002	0.959	0.007	1.007	
Pyroxene	0.14	0.38	1.088	0.004	1.150	0.003	0.946	0.005	1.011	
CTX 28										
Whole rock	0.84	2.28	1.117	0.007	1.137	0.002	0.983	0.006	1.007	
Plagioclase	0.03	0.08	1.145	0.015	1.185	0.018	0.966	0.019	1.012	
Glass	1.43	3.85	1.130	0.007	1.146	0.002	0.986	0.006	1.005	
Pyroxene	0.18	0.56	0.969	0.004	0.927	0.003	1.045	0.006	0.935	
CTX-17										
Whole rock	3.67	7.99	1.394	0.009	1.295	0.006	1.076	0.009	1.008	
Plagio clase	0.33	0.80	1.232	0.006	1.204	0.003	1.023	0.005	1.003	
Glass	3.74	8.19	1.386	0.007	1.283	0.002	1.080	0.006	1.003	
CTX 42										
Whole rock	3.21	7.51	1.295	0.009	1.262	0.002	1.026	0.007	1.002	
Plagioclase	0.17	0.49	1.047	0.006	1.087	0.008	0.963	0.009	1.011	
Glass	3.48	8.29	1.273	0.008	1.225	0.002	1.039	0.007	1.008	

All data are decay corrected.

Table 2

U–Th results for zircon grains from sample CTX-17

	$(^{238}\text{U}/^{232}\text{Th})$	$2\sigma$	$(^{230}\text{Th}/^{232}\text{Th})$	$2\sigma$	$(^{238}\text{U}/^{230}\text{Th})$	$2\sigma$
CTX zircon 1-1	4.107	0.015	3.601	0.261	1.141	0.083
CTX zircon 2-1	6.616	0.188	5.739	0.484	1.153	0.103
CTX zircon 3-1	8.716	0.069	8.242	0.820	1.058	0.106
CTX zircon 3-2	7.525	0.027	6.751	0.522	1.115	0.086
CTX zircon 4-1	6.961	0.082	6.551	1.379	1.063	0.224
CTX zircon 5-1	3.574	0.040	3.279	1.155	1.090	0.384
CTX zircon 6-1	23.735	0.351	21.270	1.453	1.116	0.078
CTX zircon 7-1	3.888	0.058	3.755	1.043	1.035	0.288

#### 4.3.2. Mineral and glass separates

Mineral and glass separates were analyzed for two of the Cotopaxi andesites (samples CTX-25 and CTX-28) and two of the Cotopaxi rhyolites (CTX-17 and CTX-42) (Table 1b). In each sample, the whole rock point lies at the end of the array with the highest  $^{238}\text{U}$  excess, and mass balance dictates the presence of a high-U phase that was not analyzed but was present in the whole rock.

**4.3.2.1. CTX-25 (andesite).** Glass and pyroxene separates have a range in  $(^{230}\text{Th})/(^{232}\text{Th})$  of 1.15–1.16, and have  $^{230}\text{Th}$  excesses of 4% (glass) to 5% (pyroxene) (Fig. 4C). A line regressed through these points and the whole rock corresponds to an age of  $28^{+1}_{-2}$  ka with an initial  $^{230}\text{Th}$  ratio of 1.16. The  $^{14}\text{C}$  eruption age for this sample is  $2.0 \pm 0.1$  ka.

**4.3.2.2. CTX-28 (andesite).** This sample represents the most recent eruption of Cotopaxi in 1877 A.D. Glass, plagioclase and pyroxene separates have a range in  $(^{230}\text{Th})/(^{232}\text{Th})$  of 0.9–1.19, and have  $^{230}\text{Th}$  excesses of 1% to 3%, with the exception of the pyroxene separate that has a  $^{238}\text{U}$  excess of 5% (Fig. 4C). This pyroxene also has a significantly low  $(^{234}\text{U})/(^{238}\text{U})$  of 0.95. A line regressed through the points has a slope of  $>1$  and therefore has no age significance.

**4.3.2.3. CTX-17 (rhyolite).** Glass and plagioclase separates from the oldest analyzed rhyolite have  $^{238}\text{U}$  excesses of 8% and 2%, respectively (Fig. 4D). An essentially two-point isochron regressed through the CTX-17 mineral data corresponds to an age of  $81.0^{+7.1}_{-6.7}$  ka, considerably older than the  $^{14}\text{C}$  eruption age of  $7270 \pm 80$  yr. The initial  $(^{230}\text{Th})/(^{232}\text{Th})$  for this array is 1.17.

**4.3.2.4. CTX-42 (rhyolite).** Glass and plagioclase separates in sample CTX-42 have a similar distribution to sample CTX-17, but the glass has a 4%  $^{238}\text{U}$  excess and the plagioclase has a  $^{230}\text{Th}$  excess of 4%. An

isochron regressed through these points corresponds to an age of  $124^{+24}_{-69}$  ka. The initial  $(^{230}\text{Th})/(^{232}\text{Th})$  for this sample is 1.16 (Fig. 4D). The age implied from U-series data is considerably older than the eruption age of  $6300 \pm 70$  yr. A line regressed through the glass and plagioclase for samples CTX-17 and CTX-42 can be fit by a single regression line, with an age of  $\sim 74$  ka that is nearly identical to the isochron formed by the rhyolite whole rocks.

#### 4.4. Zircon data

The data for zircon grains from Cotopaxi rhyolite CTX-17 (age 7ky) show that three of seven zircon grains are within error of  $(^{238}\text{U})/(^{230}\text{Th})$  secular equilibrium (Table 2, Fig. A.1<sup>2</sup>), and U–Pb dating of these zircons give Proterozoic ages of 0.8–1.2 Ga [17]. The four zircons that are out of  $(^{238}\text{U})/(^{230}\text{Th})$  equilibrium have a range in  $(^{238}\text{U})/(^{232}\text{Th})$  of 4.1–23.7. U–Pb dates obtained for the same zircons yield average Tera–Wasserburg ages [26] of 18–30 Ma [17]. The reason for the discordant zircon ages (U–Pb vs. U–Th) is most likely that the spots included very young rims on old cores. The U–Th method better detects the younger rim growth than does the U–Pb method but neither set of ages uniquely defines the timing of growth in these hybrid grains.

## 5. Discussion

### 5.1. The link between crustal thickness and assimilation

A relationship between crustal thickness and magma composition in arc rocks was noted by Plank and Langmuir [27] and by Leeman [28] who showed that crustal thickness is positively correlated with the percentage of evolved rocks (i.e., andesites, dacites and

<sup>2</sup> These data are plotted on an equiline diagram in Fig. A.1 of the online electronic supplement.

rhyolites) and with  $^{87}\text{Sr}/^{86}\text{Sr}$  of the magmatic rocks. These observations support a generally-held view that crustal assimilation plays a role in arcs where magma must traverse very thick continental crust, as in the Central Andes [29–31], although even magmas that traverse thinner crust have traces of contamination (e.g., Lesser Antilles, [31]). Crustal assimilation at Cotopaxi Volcano is evident from the presence of micro-xenoliths in the andesites and Precambrian zircon grains in the rhyolites. Assimilation is also evident in the andesites by the  $(^{234}\text{U})/(^{238}\text{U})$  of the pyroxene separate in sample CTX-28 that could only result from alteration of the pyroxene. The correlation that we have discovered between crustal thickness, nature and degree of  $^{230}\text{Th}$ – $^{238}\text{U}$  disequilibrium (Fig. 1A), suggests that there is a link between Th–U fractionation and assimilation. Given that the basic difference between island and continental arcs is not the type of sediment, fluid or lithosphere on the downgoing plate, but the thickness and type of crust of the overriding plate, it seems logical to consider the differences between thick and thin crust, and the fundamental processes that fractionate U from Th.

### 5.2. Fractionation of U from Th: source effects versus process effects

U-series disequilibria in young, volcanic arc rocks reflect either initial source melting processes or subsequent differentiation processes (i.e., source and process effects, respectively). Distinguishing between these processes is important when extracting age information. For example, U-series data are commonly used to estimate ascent rates and residence times of magma in island arcs where assimilation is shown to be negligible [5–7,32,33], a reasonable assumption in most island arcs. If, however, initial  $^{238}\text{U}$  excesses are modified by a process such as crustal assimilation, then the use of U-series data for isochrons becomes more complicated due to the assimilation and homogenization processes that take place in most continental arc volcanoes [34].  $^{238}\text{U}$  excesses are typically associated with fluid addition from the slab to the mantle wedge, however the causes of  $^{230}\text{Th}$  excesses are more complex. In terms of source processes, variable amounts of sediment and fluid addition to the mantle wedge have been used to explain  $^{230}\text{Th}$  excesses in lavas from Nicaragua [37,38], Crater Lake [39] and Alaska [21], whereas the process effects of assimilation and AFC have been used to explain  $^{230}\text{Th}$  excesses at Parinikota [11], the Cascades [9], the Himalaya [40] and the Central Andes [35].

### 5.3. Origin of $^{230}\text{Th}$ excesses in continental arc andesites

$^{230}\text{Th}$  excesses in continental arc andesites have been explained by source and process effects. In general, the range of possible processes that could generate  $^{230}\text{Th}$  excesses in arc lavas includes: 1) fractional crystallization from a mantle derived magma, of minerals that have  $D_{\text{U}} > D_{\text{Th}}$ , 2) dynamic melting of heterogeneous mantle in which  $D_{\text{U}} > D_{\text{Th}}$ , and 3) assimilation of  $^{230}\text{Th}$ -enriched crustal melts (including slab melts) by mantle derived magma. Garnet and Al-clinopyroxene preferentially retain U over Th during melting [36] and the presence of these minerals in the melting regime, lower crust or as crystallizing phases may generate  $^{230}\text{Th}$  excesses [11,36,40–45]. Alternatively, mantle heterogeneities can result from variable sediment contribution, fluid addition and mineralogical heterogeneities. Sediment input does vary from arc to arc, and it has been argued that sediment-rich sources are less sensitive to the effects of fluid addition, which results in smaller  $^{238}\text{U}$  excesses [46]. To fully assess this effect, the sediment flux of individual arcs would need to be quantified to determine if in fact the sediment input does significantly alter  $^{230}\text{Th}$  excesses. Published data show that continental arc sediments generally have lower Th concentrations and higher ( $^{238}\text{U}/^{230}\text{Th}$ ) than island arc sediments on a worldwide basis (Fig. A.2).<sup>3</sup> Regardless, the concentrations of Th and U in the mantle wedge are controlled by the conditions at the slab/mantle wedge interface (i.e., distribution coefficient values, solubilities, oxidation states) as well as by their initial concentrations in the sediment.

### 5.4. Possible causes of $^{230}\text{Th}$ – $^{238}\text{U}$ disequilibria in Cotopaxi andesites

There exist published U–Th disequilibria data for only one other NVZ volcano, Nevados del Ruiz [25]. Two andesites from that volcano have  $^{238}\text{U}$  excesses of 1–2%. In contrast, the Cotopaxi andesites range from  $^{230}\text{Th}$  excesses of 3.6% to  $^{238}\text{U}$  excesses of 6.7%. In this respect, whereas the  $^{238}\text{U}$ -enriched andesites of Cotopaxi are similar to the Nevado del Ruiz lavas, the  $^{230}\text{Th}$ -enriched andesites are more similar to the andesites from the Cascades volcanoes (e.g., Mount St. Helens, Crater Lake, Mount Shasta) in that they also have  $^{230}\text{Th}$  excesses and petrographic

<sup>3</sup> See Fig. A.2 in the online electronic supplement. Data are from Plank and Langmuir [27].

textures indicative of non-equilibrium conditions that characterize magma mixing and/or assimilation [47].

Geochemical data from Ecuadorian volcanoes suggest that melting of a garnet-bearing source contributes to the geochemical signature of NVZ lavas [48–51]. This source could be in the slab or in the Ecuadorian crust, and in fact this regional NVZ characteristic has prompted some researchers to suggest that slab melting is ubiquitous beneath most of Ecuador [52]. This is inferred on the basis of La/Yb values in the NVZ which are  $>5$ , compared with most island arcs and continental arcs with thin crust (e.g., the SVZ, New Hebrides) that have La/Yb  $<5$  [53]. Cotopaxi La/Yb values range from 7–15 (Tables A.1.a,b; Fig. 3C), however it has been pointed out that there is no evidence for a flat-slab geometry beneath Ecuador (a requirement for NVZ slab melting) and patterns in regional geochemistry are not consistent with slab melting in the NVZ [54]. In the case of Ecuador, melting of garnet-bearing lower crust is more likely to be responsible for the high La/Yb lavas. At Cotopaxi, the restricted range in trace element variation and the broad range in  $^{230}\text{Th}$  and  $^{238}\text{U}$  values make it difficult to explain these data using a single source or process. To produce the observed variation in  $^{238}\text{U}$ – $^{230}\text{Th}$  disequilibria from such a temporally narrow (ca. 6000 yr) and spatially restricted suite of volcanic rocks must require either a very heterogeneous mantle or a combination of source and process effects. Given the abundant evidence of assimilation and mixing in the Cotopaxi andesites, a multi-process hypothesis is quite reasonable. The potential effects of fractional crystallization, heterogeneous mantle melting and lower crustal assimilation on Cotopaxi U-series disequilibria are discussed below.

#### 5.4.1. Fractional crystallization

Minerals that have  $D_{\text{U}}/D_{\text{Th}} > 1$  and could produce  $^{230}\text{Th}$  excesses during crystallization are garnet, zircon and high- $\text{Al}_2\text{O}_3$  pyroxene, none of which have been observed in the Cotopaxi andesites. La/Yb values do not correlate with  $\text{SiO}_2$  content (Fig. 3C), and Zr concentrations are positively correlated with wt.%  $\text{SiO}_2$ . These observations argue against garnet fractionation and zircon precipitation, respectively, during evolution of the andesite magma suite. The andesite pyroxenes are low- $\text{Al}_2\text{O}_3$  ( $<2.0$  wt.%, [17]), which could create small  $^{238}\text{U}$  excesses during fractionation, not  $^{230}\text{Th}$  excesses [12]. Based on these observations, it is unlikely that the  $^{230}\text{Th}$  excesses in the Cotopaxi andesites are the result of crystal fractionation.

#### 5.4.2. Heterogeneous mantle

Most trace element variations in continental arc andesites can be explained by differentiation processes [55], however mantle heterogeneities have been inferred from some data sets, as is the case in Nicaragua [56,38]. Mantle wedge heterogeneities are typically recognized by variable HFSE ratios within a suite of volcanic rocks. In fact, the trace element data for Cotopaxi Volcano reflect limited compositional variation throughout 6000 yr of eruptive history; Ti/Zr, Nb/Y and other HFSE ratios in the Cotopaxi andesites are not significantly fractionated (Fig. 3B). The Cotopaxi  $^{87}\text{Sr}/^{86}\text{Sr}$  and  $^{143}\text{Nd}/^{144}\text{Nd}$  values are nearly identical for all the analyzed samples, which also argues against long-lived source heterogeneity [17], although U–Th isotopes may reflect recent modifications to the mantle wedge that are independent of Sr and Nd isotopes. Taken together, these data suggest that mantle variations are either effectively homogenized during ascent and storage, which would not explain the variable  $(^{230}\text{Th})/(^{238}\text{U})$  values, or not initially imparted to the mantle-derived magmas.

#### 5.4.3. Assimilation of crust or crustal melts

Regional studies of  $\delta^{18}\text{O}$  and Sr isotope data from the NVZ are consistent with up to  $\sim 20\%$  assimilation of mafic crust [57,58], and the average Cotopaxi  $^{87}\text{Sr}/^{86}\text{Sr}$  of 0.70420 [17] in the rhyolites and andesites is permissive of assimilation of a mafic or juvenile component. Bulk addition of crust would not be expected to create disequilibria since  $(^{238}\text{U})/(^{230}\text{Th})=1$  in crust  $>350$  ka old, so assimilation would create disequilibrium only if the assimilant is a  $^{230}\text{Th}$  or  $^{238}\text{U}$ -enriched partial melt. Formation of a  $^{230}\text{Th}$ -enriched partial melt requires anatexis of a lithology that has a refractory phase that retains U over Th, i.e., garnet, Al-rich clinopyroxene or accessory phases (i.e., zircon, allanite).

There are many crustal lithologies that typify the Ecuadorian crust, however on the basis of age and radiogenic Sr isotope ratios, only a few are considered as candidates for assimilation. These include the accreted mafic rocks of the Macuchi island arc terrain, and the eclogite/garnet amphibolite lithologies similar to that of the Rapsas UHP terrain (Fig. 1). Numerical models have shown that underplating of basalt provides sufficient heat to induce melting of the lower crust [59–62], and it has been shown that  $^{230}\text{Th}$  excesses can be generated in mafic magmas by melting of garnet-bearing lithologies. [40,43]. Although some models of lower crustal melting show that high melt fractions (10–40%) do not generate significant  $^{230}\text{Th}$  excesses [45], at degrees of partial melting less than 10%, the degree of  $^{230}\text{Th}$  enrichment increases significantly.

### 5.5. Modeling of $^{230}\text{Th}$ – $^{238}\text{U}$ disequilibria in Cotopaxi andesite

To test the hypothesis that lower crustal melting could create  $^{230}\text{Th}$  excesses in the Cotopaxi rocks, equilibrium melting calculations were used to model melting of four lower crustal lithologies of the Raspas UHP complex: eclogite, amphibolite, garnet amphibolite and metapelitic garnet-schist. Thermobarometry measurements on minerals in the Raspas UHP terrain give maximum pressures of nearly 2.0 GPa (~60 km) [20]. This terrain has Sr isotope values of 0.70306–0.70649 [19,20], which makes it a good candidate for an assimilant in the NVZ. This outcrop contains 80% metapelitic garnet-schist and 20% garnet amphibolite, amphibolite and eclogite. Accessory zircon and apatite have been reported in the metapelitic schist. Pyroxenes from the Raspas eclogite are high- $\text{Al}_2\text{O}_3$  (~9–15 wt.%) [20] and therefore would have  $D_{\text{U}}/D_{\text{Th}} > 1$  at pressures that pertain to the lower crust (60 kbar).

Distribution coefficients ( $D$  values) and mineral proportions for batch melting calculations are taken from published literature [63–66], and are given in Table 3a. Melting curves plotted in Fig. 5 illustrate  $^{238}\text{U}$  and  $^{230}\text{Th}$  excesses versus degree of melting.

Table 3a  
Modal proportions<sup>a</sup> and  $D$  values for lithologies used in melting calculations

Mineralogy	Modal %	$D_{\text{U}}$	$D_{\text{Th}}$
<b>Pelitic schist</b>			
Quartz	68	0	0
Garnet	11	0.023	0.01
Phengite	21		
<b>Eclogite</b>			
Garnet	27	0.023	0.01
Pyroxene	39	0.0007	0.0015
Amphibole	23	0.007	0.022
Apatite	0.2	0.01	1.6
Others	10.8		
<b>Garnet amphibolite</b>			
Garnet	10	0.023	0.01
Amphibole	50	0.007	0.022
Zoisite	30		
Omphacite	10		
<b>Amphibolite</b>			
Amphibole	40	0.007	0.022
Plagioclase	60	0.001	0.001

Distribution coefficient values and mineral proportions used for modeling lower crustal melting of the Raspas UHP complex. Distribution coefficients are from [64–66]. These values are given in Fig. 6B.

<sup>a</sup> Feininger, 1980 [76].

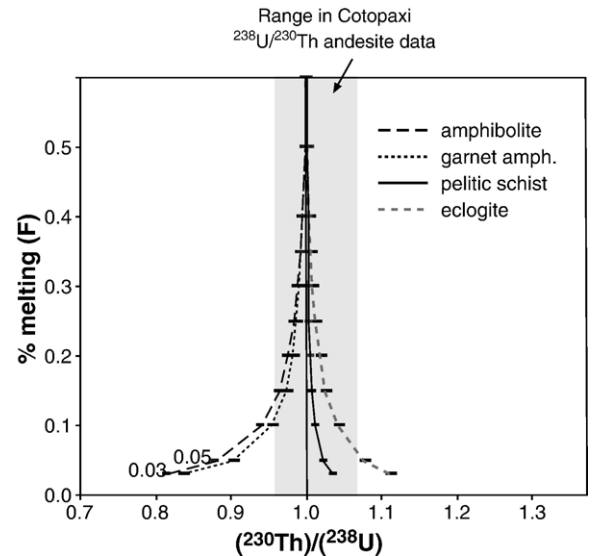


Fig. 5. Model of lower crustal melting, using four lithologies of the Raspas UHP terrain, and showing  $F$  (% melt) vs.  $(^{238}\text{U})/(^{230}\text{Th})$ . Distribution coefficients (Table 3a) are from [64–66]. The gray shaded region represents the total observed range in  $(^{238}\text{U})/(^{230}\text{Th})$  for the Cotopaxi andesites.  $^{230}\text{Th}$  excesses are produced by melting of pelitic schist and eclogite lithologies, whereas  $^{238}\text{U}$  excesses are produced by melting of amphibolite and garnet amphibolite lithologies.

Melting of eclogite produces the highest  $^{230}\text{Th}$  excesses, up to 13% at 3% melt, whereas melting of pelitic schist produces  $^{230}\text{Th}$  excesses of up to 5%. On the basis of this modeling, we propose that low degree (3–10%) melting of eclogitic lower crust can generate  $^{230}\text{Th}$  excesses, and that these excesses may partially overprint initial fluid-imparted  $^{238}\text{U}$  excesses. Melting of garnet amphibolite and amphibolite, on the other hand, produce  $^{238}\text{U}$  excesses of up to 20%. Interestingly, this suggests that some degree of  $^{238}\text{U}$  excess in arcs can be produced by lower crustal melting and not solely by fluid addition to the mantle wedge. Lack of a correlation between U/Th and  $\text{SiO}_2$  content among the Cotopaxi andesites (Fig. 3B) rules out simple mixing between  $^{238}\text{U}$ -enriched magma and  $^{230}\text{Th}$ -enriched lower crustal melts, however it is likely that  $\text{SiO}_2$  contents have been subsequently modified during ascent and crystallization.

In summary, it is concluded that there is minimal evidence for heterogeneous mantle melting in the Cotopaxi andesites, and that mineral fractionation is unlikely to produce the observed U–Th variation. Alternatively, lower crustal melting of eclogite and garnet-bearing pelitic schist can account for the observed range of  $^{238}\text{U}$ – $^{230}\text{Th}$  values in the Cotopaxi lavas.

5.6. Source of  $^{238}\text{U}$  excesses in the Cotopaxi rhyolite

Most arc rhyolites have equilibrium values or  $^{238}\text{U}$  excesses of only a few percent (Fig. 1D, [39]), which makes the  $^{238}\text{U}$  excesses of 4–14% in the Cotopaxi rhyolites seem unusually high. These excesses are higher than those of the Cotopaxi andesites, which rules out closed system crystallization of the rhyolite from  $^{230}\text{Th}$ -enriched Cotopaxi andesites, despite the fact that the rhyolites and andesites have the same  $^{87}\text{Sr}/^{86}\text{Sr}$  values of 0.70420. Fluid addition at a later stage of rhyolite formation (i.e.,  $^{238}\text{U}$ -rich meteoric water) is unlikely on the basis of the fluid sensitive element ratio Ba/Th that is lower in the rhyolites than in the andesites (Fig. 3D inset). The presence of accessory allanite and apatite in the rhyolite points to a possible mechanism for generating  $^{238}\text{U}$

excesses, since both minerals retain Th over U during crystallization.

It has been shown that the high  $D$  values of accessory phases in rhyolitic melt allow for significant U–Th fractionation by small quantities ( $\ll 1\%$ ) of accessory minerals [66]. Both allanite and apatite are visible in thin section, and fractionation of apatite is evidenced by an inverse correlation between  $\text{P}_2\text{O}_5$  and  $\text{SiO}_2$  (Table A.1.). Trace element trends are consistent with 70–80% crystallization of an assemblage containing  $<0.05\%$  apatite (Fig. 6A). Raleigh crystallization models were used to calculate  $^{238}\text{U}$  excesses produced by fractionation of apatite and allanite, using  $D$  values listed in Table 3b. On the basis of petrographic analyses and SEM imaging, the collective percentage of apatite, zircon and allanite in the Cotopaxi rhyolite is estimated to be  $\sim 0.051\%$  by volume. Fractionation curves were

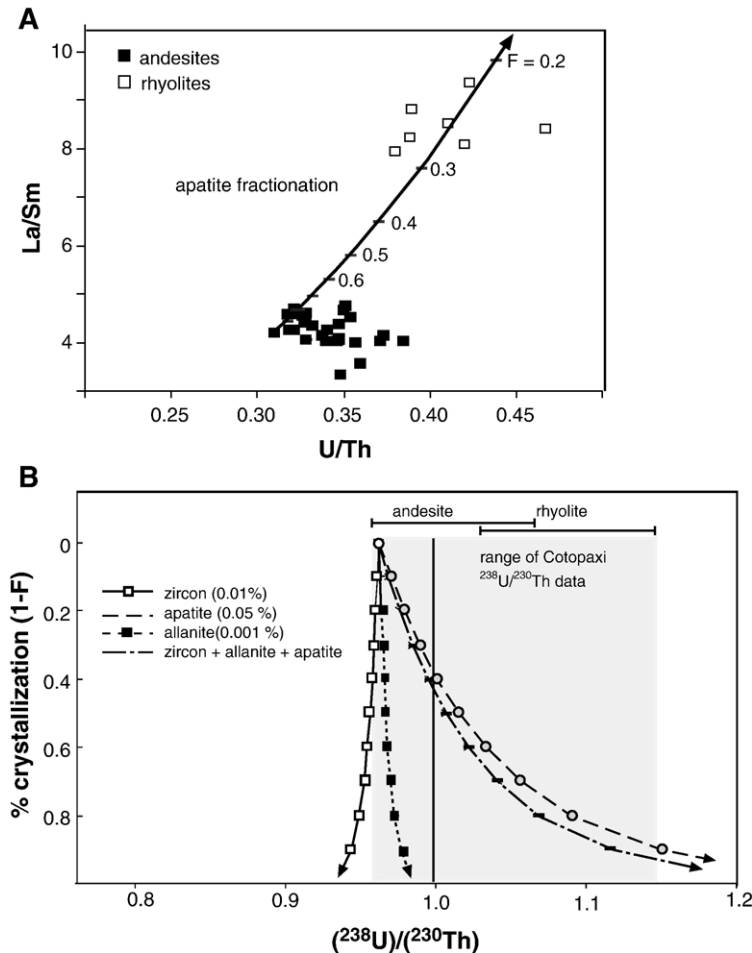


Fig. 6. (A) Graph of U/Th versus La/Sm. This shows that the majority of the Cotopaxi rhyolites (white squares) can be produced by fractionation of 40–80% crystallization from the lowest U/Th andesite. (B) Modeled variation in  $(^{238}\text{U})/(^{230}\text{Th})$  with  $F$  (% melt) during crystallization of zircon, apatite and allanite.  $D$  values are from [63–65]. The gray shaded region represents the observed  $(^{238}\text{U})/(^{230}\text{Th})$  range in the Cotopaxi data.  $D$  values are listed in Table 3b.

Table 3b  
D values of minerals used in Rayleigh fractionation calculations

Mineral	$D_U$	$D_{Th}$
Apatite	1.8	17
Zircon	100	16
Allanite	12	648
Quartz	0	0
Amphibole	0.102	0.26
Plagioclase	0.001	0.001

Distribution coefficient values and mineral proportions used for modeling fractionation of allanite and apatite to produce the  $^{238}U$  excesses in the Cotopaxi rhyolite. Distribution coefficients are from [64–66]. The modal proportions for the rhyolite calculations vary depending on the model curve. These values are given in Fig. 6B.

modeled for apatite, allanite and zircon, as well as combinations of zircon+apatite and zircon+apatite+allanite (Fig. 6B). These curves show that 30–90% crystallization of the assemblage allanite (0.001%)+apatite (0.05%)+plagioclase, quartz, biotite and magnetite (99.949%) is required to generate the range of  $^{238}U$  excesses in the rhyolites, while simultaneously reproducing major and trace element compositions [17].

In summary, the  $^{238}U$  excesses observed in the Cotopaxi rhyolites are unlikely to be the result of fluid addition or differentiation of parental  $^{238}U$ -enriched andesites. Crystallization models show that the observed range in  $^{238}U$  excesses can be explained by fractionation of apatite and allanite from rhyolitic melt.

### 5.7. Cotopaxi whole rock isochrons: age significance?

Whole rock isochrons potentially reflect the time between U–Th fractionation and eruption under ideal closed system conditions, however research on continental arc volcanoes has shown that linear arrays on equiline diagrams may represent mixing lines between different generations of magma batches, crystals or cumulate material (Mt. Shasta, [9]; Mount St. Helens, [67]), or cryptic assimilation [39]. The slope of the Cotopaxi andesite whole rock data on the equiline diagram corresponds to an apparent age of  $78^{+8.0}_{-7.5}$  ka (Fig. 4A), however there is strong evidence in the Cotopaxi andesites for open system processes (micro-xenoliths, enclaves, mineral textures). Because of this it may not be practical to determine an ascent rate from the andesite data, although we can say with certainty that assimilation happened less than 350 ka ago. There is a contradiction between the slope of the  $^{230}Th$  apparent isochron<sup>4</sup> (Fig.

<sup>4</sup> We use the term “apparent isochron” to infer that although the data form an array and it is possible to calculate an age, this age may not have age significance due to open system processes.

4A) and the presence of  $^{226}Ra$  excesses (Fig. 4B), which can be reconciled if the andesite whole rock array is not attributed to ageing, but instead to magma mixing or assimilation of a lower crustal melt.

The rhyolite whole rocks form a more pronounced isochron on the equiline diagram (albeit this is on the basis of essentially two points) than the andesite group (Fig. 4A). The presence of Precambrian zircon indicates that crustal assimilation played a role in magmagenesis; whether by assimilation of crust before or during rhyolite formation is not clear. If the whole rocks are considered as an isochron, it corresponds to a residence time of  $74^{+5.5}_{-5.2}$  ka since formation of allanite and apatite. This timeframe is not unreasonable for rhyolite from continental arc volcanoes [22,69], and could in fact be an underestimate if crystallization was protracted.

### 5.8. Cotopaxi mineral isochrons

Mineral isochrons should reflect the age of crystals that formed in a batch of magma, which may in turn reflect the residence time of that particular batch of magma in the crust. As already noted, apparent isochrons can result from mixing between crystals from new and old magma batches and entrainment of cumulate material [67,68].

#### 5.8.1. Andesites

Of the two mineral isochrons from the Cotopaxi andesites, only one could have age significance: sample CTX-25 reflects an apparent isochron age of  $28^{+13}_{-12}$  ka (glass, pyroxene, whole rock), greater than the eruption age of 2050 yr (Fig. 4C). Given the textural evidence for assimilation and mixing, it is quite likely that this linear array reflects mixed age populations of plagioclase and pyroxene with older re-entrained crystals and granulite fragments. This may also explain why the pyroxene from andesite CTX-28 has lower  $(^{230}Th)/(^{232}Th)$  than the whole rock, and a  $(^{234}U)/(^{238}U)$  of 0.95 that can only result from alteration and re-entrainment of these crystals. The  $\delta^{18}O$  value of  $6.49 \pm 0.42\%$  for sample CTX-25 is elevated above upper mantle values ( $\sim +5.5\%$ ; [70]), consistent with assimilation of crust.

#### 5.8.2. Rhyolites

Mineral and glass isochrons for two of the Cotopaxi rhyolites give ages of  $76 \pm 4$  ka (CTX-17) and  $112^{+15}_{-13}$  ka (CTX-19), much greater than their respective eruption ages of 7.2 and 6.3 ka (Fig. 4D). CTX-17 is within error of the whole rock isochron age of  $\sim 74$  ka. These isochrons potentially reflect residence times of  $\sim 70$ –

100ka, assuming that any significant crustal assimilation took place prior to crystallization of plagioclase in the rhyolite, and that the plagioclase crystals are in equilibrium with the glass. It is interesting that the plagioclase, glass and whole rocks from both samples fall along the same line, which implies that they could have crystallized from the same magma. If contamination is minimal or does not appreciably change the  $(^{230}\text{Th})/(^{232}\text{Th})$  of the rhyolite, then these isochrons may indeed represent differentiation/assimilation times of the rhyolite on the order of 70–100ka. This would represent the minimum residence time since the precipitation of major mineral phases. Longer residence times for large volume magma chambers are not unknown; it has been shown that rhyolite in very large

systems may “reside” in the crust for as long as 200–300ka [22,69,71]. Thus, the rhyolite mineral isochrons are believed to represent approximate residence times of  $\sim 10^4$ – $10^5$  yr.

### 6. Petrogenetic model

The U-series characteristics of the Cotopaxi rocks leads to our proposed petrogenetic model of 1) lower crustal melting and assimilation, followed by 2) generation of the rhyolites by crystal fractionation (Fig. 7).

- 1). Low to moderate degree (<20%) melting of eclogite or pelitic schist in the lower crust

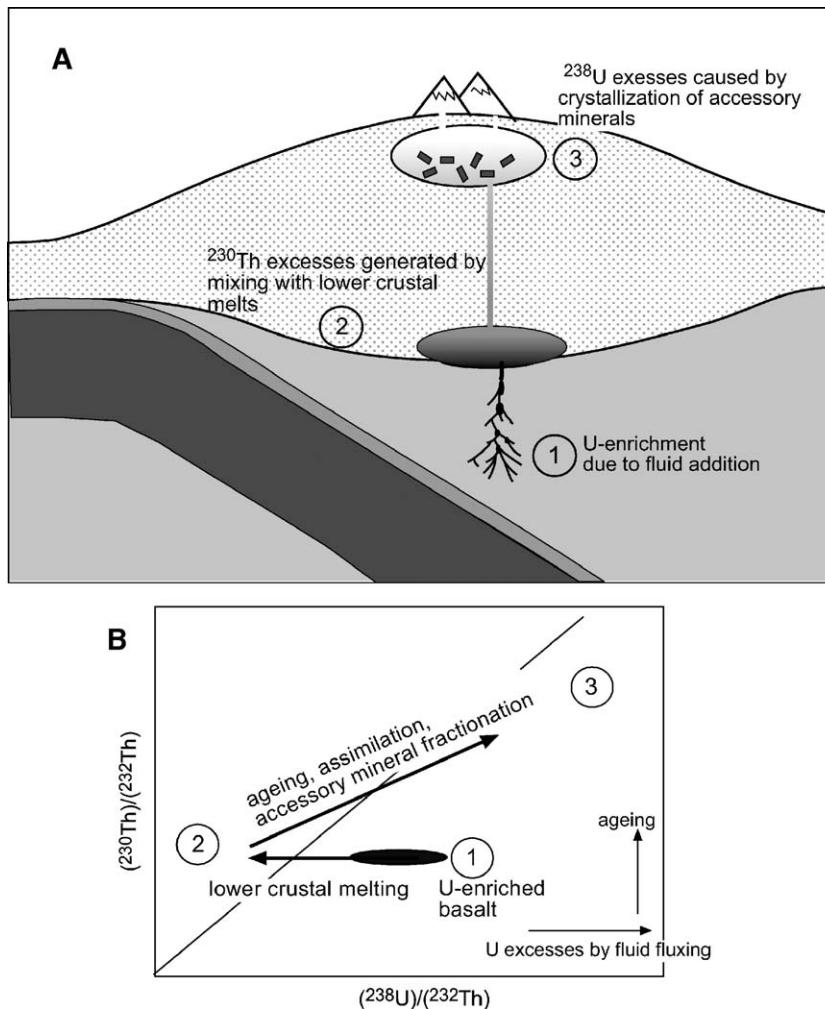


Fig. 7. (A) Petrogenetic model illustrating multi-level open system processes at Cotopaxi Volcano. Mantle wedge magmas with initial  $^{238}\text{U}$  excesses (step 1) assimilate lower crustal melts that have  $^{230}\text{Th}$  excesses (step 2). This creates the range of  $^{238}\text{U}$  and  $^{230}\text{Th}$  excess in the andesite. Crystallization of accessory phases during rhyolite formation in the upper crust creates  $^{238}\text{U}$  excesses in the rhyolites (step 3). (B) Schematic illustration of the effects of steps 1, 2 and 3 on the equiline diagram.

generates magmas that have  $^{230}\text{Th}$  excesses. Mixing of these melts with mantle wedge basalt overprints mantle-derived  $^{238}\text{U}$  excesses and creates the observed range of  $^{238}\text{U}$  and  $^{230}\text{Th}$  values in the Cotopaxi andesites.  $^{226}\text{Ra}$  excesses in the andesites also suggest that the linear array defined by the andesite whole rock data is better explained by mixing and not solely by ageing. If the  $^{226}\text{Ra}$  excess is due to fluid addition from the slab, then this puts a constraint on the time from fluid addition of <8000 yr [72]. On the other hand, if the  $^{226}\text{Ra}$  excess is due to lower crustal melting (i.e., amphibole dehydration, [73]) then the timing of lower crustal assimilation can be similarly constrained. On the basis of glomerocryst mineralogy, early differentiation in the andesite was dominated by pyroxene and plagioclase fractionation. Fragments of metamorphic rock (micro-xenoliths) in the least evolved andesites are consistent with assimilation of crust. Pervasive resorption textures in the plagioclase grains are evidence for repeated episodes of mixing and recharge.

- 2). As the andesite magma ascends, differentiation occurs through crystallization of plagioclase, amphibole, quartz, magnetite, biotite and the accessory phases apatite, allanite, and zircon. After approximately 60–90% crystallization, precipitation of apatite and allanite generates  $^{238}\text{U}$  excesses in the Cotopaxi rhyolites. The high  $D_{\text{Th}}/D_{\text{U}}$  of apatite and allanite produces the observed  $^{238}\text{U}$  excesses of up to 14%. On the basis of the mineral and whole rock data, the time scale of rhyolite formation at Cotopaxi is on the order of 70–100 ka. Furthermore, similarities in the slopes between the rhyolite whole rock and mineral isochrons suggest that the eruptions may be related to the same batch of magma. If this is the case, the occurrence of punctuated rhyolite eruptions from a single magma chamber would be required.

## 7. Summary and conclusions

The U-series data from Cotopaxi Volcano are consistent with a petrogenetic model of multi-level differentiation that includes lower crustal melting and assimilation of eclogite and/or garnet-bearing pelitic schist followed by rhyolite formation and preferential retention of Th by accessory mineral phases. Evident open system processes in the andesite (i.e., entrainment of cumulates and mixing of crystal populations) do not

permit for age information to be extracted from the equiline diagram, however the  $^{226}\text{Ra}$  excesses are consistent with a time scale for assimilation and ascent of the andesite of <8000 yr. The onset of accessory phase fractionation during formation of the rhyolite creates  $^{238}\text{U}$  excesses of 4–14%. On the basis of the whole rock and mineral data, an approximate residence time for the rhyolite is inferred to be on the order of ~75–100 ka.

When considered in the context of this model, the correlation between crustal thickness and sense of disequilibrium may reflect the modification of mantle melts by lower crustal melting of pelitic schist or eclogite facies rock. This is not to say that lower crustal melting occurs at all arcs with thick crust, or that mantle garnet does not contribute to  $^{230}\text{Th}$  excesses in other arcs. Indeed, magma composition depends on a wide range of variables, some of which will create U-series disequilibria. There is a global correlation between  $^{238}\text{U}$  excess and crustal thickness, and we suggest in a general sense that this correlation is linked to crustal processes. Lower crustal melting and assimilation is one process that can account for this trend, and at Cotopaxi Volcano, there is little evidence for mantle heterogeneity and reasonable evidence for lower crustal residual garnet. The results of this research have important implications for interpreting U-series data in continental arcs, including: 1)  $^{230}\text{Th}$  excesses in continental arc andesites can be generated by small degrees of lower crustal melting and assimilation that is consistent with previous numerical modeling and 2)  $^{238}\text{U}$  excesses in rhyolites may be caused by accessory phase fractionation, rather than being inherited from parents which have  $^{238}\text{U}$  excesses from fluid addition to the mantle wedge.

## Acknowledgements

We gratefully acknowledge Rhiannon George, Tim Elliott and the rest of the isotope geochemistry group at the University of Bristol for use of the lab facilities and valuable discussions of the U-series data. We also thank Dave Matthey and Dave Lowe at UC London for their assistance with oxygen isotope analyses, and the grad students and staff at the GeoAnalytical Lab at WSU for conducting the ICP and XRF analyses. We also thank Pete Hall and Patricia Mothes from the Instituto de Geofisico in Quito, Ecuador for providing the Cotopaxi stratigraphy, field assistance and research insights. Improvements were made on the basis of reviews by Kari Cooper and Bernard Bourdon and discussions with Mark Reagan. Funds were provided

by NSF Grant EAR 9980407, a GSA student research grant and the UCLA Latin American Studies program. Garrison acknowledges receipt of a UCLA Dissertation Year fellowship.

## Appendix A. Supplementary data

Supplementary data associated with this article can be found, in the online version, at [doi:10.1016/j.epsl.2006.02.013](https://doi.org/10.1016/j.epsl.2006.02.013).

## References

- [1] J.B. Gill, R.W. Williams, Th isotope and U-series studies of subduction-related volcanic rocks, *Geochim. Cosmochim. Acta* 54 (1990) 1427–1442.
- [2] S. Turner, B. Bourdon, J. Gill, Insights into magma genesis at convergent margins from U-series isotopes, in: Bourdon, Henderson, Lundstrom, Turner (Eds.), *Uranium-Series Geochemistry*, vol. 52, 2003, pp. 255–315.
- [3] S. Turner, C. Hawkesworth, Constraints on flux rates and mantle dynamics beneath island arcs from Tonga–Kermadec lava geochemistry, *Nature* 389 (1997) 568–573.
- [4] T. Elliott, T. Plank, A. Zindler, W. White, B. Bourdon, Bernard, Element transport from slab to volcanic front at the Mariana Arc, *J. Geophys. Res.* 102 (1997) 14,991–15,019.
- [5] S. Turner, C. Hawkesworth, N. Rogers, J. Bartlett, T. Worthington, J. Hergt, J. Pearce, I. Smith,  $^{238}\text{U}$ – $^{230}\text{Th}$  disequilibria, magma petrogenesis, and flux rates beneath the depleted Tonga–Kermadec island arc, *Geochim. Cosmochim. Acta* 61 (1997) 4855–4884.
- [6] S.P. Turner, R.M. George, P.J. Evans, C.J. Hawkesworth, G.F. Zellmer, Timescales of magma formation, ascent and storage beneath subduction-zone volcanoes, *Philos. Trans. R. Soc. Lond.* 358 (2000) 1443–1464.
- [7] C.J. Hawkesworth, S.P. Turner, F. McDermott, D.W. Peate, P. van Clasteren, U–Th isotopes in arc magmas: implications for element transfer from subducted crust, *Science* 276 (1997) 551–555.
- [8] C. Allegre, M. Condomines, Fine chronology of volcanic processes using  $^{238}\text{U}$ – $^{230}\text{Th}$  systematics, *Earth Planet. Sci. Lett.* 28 (1976) 395–406.
- [9] A.M. Volpe,  $^{238}\text{U}$ – $^{230}\text{Th}$ – $^{226}\text{Ra}$  disequilibrium in young Mt. Shasta andesites and dacites, *J. Volcanol. Geotherm. Res.* 53 (1992) 227–238.
- [10] A.M. Volpe, P. Hammond,  $^{238}\text{U}$ – $^{230}\text{Th}$ – $^{226}\text{Ra}$  disequilibria in young Mount St. Helens rocks: time constraint for magma formation and crystallization, *Earth Planet. Sci. Lett.* 107 (1991) 475–486.
- [11] B. Bourdon, B.G. Worner, A. Zindler, U-series evidence for crustal involvement and magma residence times in the petrogenesis of Parinacota Volcano, Chile, *Contrib. Mineral. Petrol.* 139 (2000) 458–469.
- [12] B.J. Wood, J.D. Blundy, J. Robinson, C. Andrew, The role of clinopyroxene in generating U-series disequilibrium during mantle melting, *Geochim. Cosmochim. Acta* 63 (1999) 1613–1620.
- [13] A. Heumann, G.R. Davies, T. Elliott, Crystallization history of rhyolites at Long Valley, California, inferred from combined U-series and Rb–Sr isotope systematics, *Geochim. Cosmochim. Acta* 66 (2002) 1821–1837.
- [14] B. Bourdon, S. Turner, G. Henderson, M. Gideon, C. Lundstrom, Introduction to U-series geochemistry, in: Bourdon, Henderson, Lundstrom, Turner (Eds.), *Uranium-Series Geochemistry*, vol. 52, 2003, pp. 1–21.
- [15] M. Ivanovich, R.S. Harmon, *Uranium Series Disequilibrium: Applications to Earth, Marine and Environmental Sciences*, Clarendon Press, Oxford, 1992.
- [16] F. Barberi, M. Coltelli, A. Frullani, M. Rosi, E. Almeida, Chronology and dispersal characteristics of recently (last 5000 years) erupted tephra of Cotopaxi (Ecuador): implications for long term eruptive forecasting, *J. Volcanol. Geotherm. Res.* 69 (1995) 17–239.
- [17] J.M. Garrison, Magmatic processes at Cotopaxi Volcano, Ecuador: geochemical and petrological constraints, and inferences for continental arc volcanoes, Univ. of California, Los Angeles, Dissertation (2004) 247 pp.
- [18] T. Feininger, M.K. Seguin, Simple Bouguer gravity anomaly field and the inferred crustal structure of continental Ecuador, *Geology* 11 (1983) 40–44.
- [19] R.J. Arculus, H. Lapiere, E. Jaillard, A geochemical window into subduction–accretion processes: the Raspas Metamorphic Complex, Ecuador, *Geology* 27 (1999) 547–550.
- [20] D. Bosch, G. Piercarlo, H. Henritec, J.-L. Malfere, J. Etienne, Geodynamic significance of the Raspas Metamorphic Complex (SW Ecuador): geochemical and isotopic constraints, *Tectonophysics* 345 (2002) 83–102.
- [21] R. George, S. Turner, C. Hawkesworth, C. Bacon, C. Nye, P. Stelling, S. Dreher, Chemical versus temporal controls on the evolution of tholeiitic and calc-alkaline volcanoes in the Alaska–Aleutian arc, *J. Petrol.* 45 (2003) 203–219.
- [22] M.R. Reid, C.D. Coath, M.T. Harrison, K.D. McKeegan, Prolonged residence times for the youngest rhyolites associated with Long Valley Caldera:  $^{230}\text{Th}$ – $^{238}\text{U}$  ion microprobe dating of young zircons, *Earth Planet. Sci. Lett.* 150 (1997) 27–39.
- [23] G. Dalrymple, M. Grove, O.H. Lovera, T.M. Harrison, J.B. Hulen, M.A. Lanphere, Age and thermal history of the Geysers plutonic complex (felsite unit), Geysers geothermal field, California: a  $^{40}\text{Ar}/^{39}\text{Ar}$  and U–Pb study, *Earth Planet. Sci. Lett.* 173 (1999) 285–298.
- [24] U. Schaerer, The effect of initial  $^{230}\text{Th}$  disequilibrium on young U–Pb ages: the Makalu case, Himalaya, *Earth Planet. Sci. Lett.* 67 (1984) 191–204.
- [25] S.J. Schaefer, N.C. Sturchio, M.T. Murrell, S.N. Williams, Internal  $^{238}\text{U}$ -series systematics of pumice from the November 13, 1985, eruption of Nevado del Ruiz, Colombia, *Geochim. Cosmochim. Acta* 57 (1983) 1215–1219.
- [26] F. Tera, G.J. Wasserburg, U–Th–Pb systematics on lunar rocks and inferences about lunar evolution and the age of the moon, Proceedings from the 5th Lunar Science Conference (Supplement 5), *Geochim. Cosmochim. Acta*, vol. 2, 1974, pp. 1571–1599.
- [27] T. Plank, C.H. Langmuir, The chemical composition of subducting sediment and its consequences for the crust and mantle, *Chem. Geol.* 145 (1998) 325–394.
- [28] W.P. Leeman, The influence of crustal structure on compositions of subduction-related magmas, in: S. Aramaki, I. Kushiro (Eds.), *Arc Volcanism: J. of Volcanol. Geotherm. Res.*, vol. 18, 1983, pp. 561–588.
- [29] J.P. Davidson, N.J. McMillan, S. Moorbath, G. Worner, R.S. Harmon, L. Lopez-Escobar, The Nevados de Payachata volcanic

- region (18°S, 69°W, N. Chile): II. Evidence for widespread crustal involvement in Andean magmatism, *Contrib. Mineral. Petrol.* 105 (1990) 412–432.
- [30] N.J. McMillan, J.P. Davidson, G. Worner, R.S. Harmon, S. Moorbath, L. Lopez-Escobar, Influence of crustal thickening on arc magmatism: Nevados de Payachata volcanic region, northern Chile, *Geology* 21 (1993) 467–470.
- [31] J. Davidson, Crustal contamination versus subduction zone enrichment: examples from the Lesser Antilles and implications for mantle source compositions of island arc volcanics. *Geochim. Cosmochim. Acta*, v. 51, pp. 2185–2198.
- [32] S. Turner, F. McDermott, C. Hawkesworth, P. Kepezhinskis, A U-series study of lavas from Kamchatka and the Aleutians: constants on source composition and melting processes, *Contrib. Mineral. Petrol.* 133 (1998) 217–234.
- [33] S. Turner, J. Foden, R. George, P. Evans, R. Varne, M. Elburg, G. Jenner, George, Rates and processes of potassic magma evolution beneath Sangeang Api Volcano, east Sunda Arc, Indonesia, *J. Petrol.* 44 (2003) 491–515.
- [34] B. Deruelle, R.S. Harmon, S. Moorbath, Combined Sr–O isotope relationships and petrogenesis of Andean volcanics of South America, *Nature* 302 (1983) 814–816.
- [35] Hildreth, S. Moorbath, Crustal contributions to arc magmatism in the Andes of Central Chile, *Contrib. Mineral. Petrol.* 98 (1988) 455–499.
- [36] J.D. Blundy, Heavy REE are compatible in clinopyroxene on the spinel lherzolite solidus, *Earth Planet. Sci. Lett.* 160 (1998) 493–504.
- [37] M.K. Reagan, J.B. Gill, Coexisting calc-alkaline and high Nb basalts from Turrialba Volcano, Costa Rica, implications for residual titanites in arc magma sources, *J. Geophys. Res.*, B 94 (1989) 4619–4633.
- [38] R.B. Thomas, M.M. Hirschmann, H. Cheng, M.K. Reagan, L.R. Edwards, ( $^{231}\text{Ra}/^{235}\text{U}$ )–( $^{230}\text{Th}/^{238}\text{U}$ ) of young mafic volcanic rocks from Nicaragua and Costa Rica and the influence of flux melting on U-series systematics of arc lavas, *Geochim. Cosmochim. Acta* 66 (2002) 4287–4309.
- [39] M.K. Reagan, K.W. Sims, J. Erich, R.B. Thomas, H. Cheng, R.L. Edwards, G. Layne, L. Ball, Timescales of differentiation from mafic parents to rhyolite in North American continental arcs, *J. Petrol.* 44 (2003) 1703–1726.
- [40] J. Dufek, K.M. Cooper,  $^{226}\text{Ra}/^{230}\text{Th}$  excess generated in the lower crust: implications for magma transport and storage timescales, *Geology* 33 (2005) 833–836.
- [41] D. McKenzie,  $^{230}\text{Th}$ – $^{238}\text{U}$  disequilibrium and the melting processes beneath ridge axes, *Earth Planet. Sci. Lett.* 72 (1985) 149–157.
- [42] R. Williams, J. Gill, Effects of partial melting on the uranium decay series, *Geochim. Cosmochim. Acta* 53 (1989) 1607–1619.
- [43] K.M. Cooper, M.R. Reid, N.W. Dunbar, W.C. McIntosh, Origin of mafic magmas beneath northwestern Tibet: constraints from  $^{230}\text{Th}$ – $^{238}\text{U}$  disequilibria, *Geochem. Geophys. Geosyst.* 3 (2002) 1525–2027.
- [44] O. Sigmarsson, H. Martin, J. Knowles, Melting of a subducting oceanic crust from U–Th disequilibria in Austral Andean lavas, *Nature* 394 (1998) 566–569.
- [45] K. Berlo, S. Turner, J. Blundy, C. Hawkesworth, The extent of U-series disequilibria produced during partial melting of the lower crust with implications for the formation of the Mount St. Helens dacites, *Contrib. Mineral. Petrol.* 148 (2004) 122–130.
- [46] R. George, S. Turner, C. Hawkesworth, J. Morris, C. Nye, J. Ryan, S. Zheng, Melting processes and fluid and sediment transport rates along the Alaska–Aleutian arc from an integrated U–Th–Ra–Be isotope study, *J. Geophys. Res.* 108 (2003) 2252.
- [47] S. Newman, D.J. Maccougall, R.C. Finkel, Petrogenesis and  $^{230}\text{Th}$ – $^{238}\text{U}$  disequilibrium at Mt. Shasta, California, and in the Cascades, *Contrib. Mineral. Petrol.* 93 (1986) 195–206.
- [48] P. Samaniego, H. Martin, C. Robin, M. Monzier, Transition from calc-alkalic to adakitic magmatism at Cayambe Volcano, Ecuador: insights into slab melts and mantle wedge interactions, *Geology* 30 (2002) 967–970.
- [49] E. Bourdon, M.F. Thirwall, M. Monzier, P. Samaniengo, J.-P. Eissen, C. Robin, Isotopic Zoning of the NVZ in Ecuador: Implications for Magma Sources and Petrogenetic Processes, Abstracts with Programs, AGU-EGS Meeting, Nice, France, 2003, p. 494.
- [50] M. Monzier, C. Robin, P. Samaniego, M.L. Hall, J. Cotten, P. Mothes, N. Arnaud, Sangay Volcano, Ecuador: structural development, present activity and petrology, *J. Volcanol. Geotherm. Res.* 90 (1990) 49–79.
- [51] P. Starr, Geology and petrology of Ruminahui Volcano, Ecuador [Masters Thesis], (1984) University of Oregon, 98 pp.
- [52] M.-A. Gutscher, R. Maury, J.-P. Eissen, E. Bourdon, Can slab melting be caused by flat subduction? *Geology* 28 (2000) 535–538.
- [53] M.J. Defant, M.S. Drummond, Derivation of some modern arc magmas by melting of young subducted lithosphere, *Nature* 347 (1990) 662–665.
- [54] J.M. Garrison, J.P. Davidson, Dubious case for slab melting in the Northern Volcanic Zone, Ecuador, *Geology* 28 (2003) 316–320.
- [55] J.P. Davidson, R.S. Harmon, G. Worner, The source of central Andean magmas; some considerations, *GSA Spec. Pap.* 265 (1991) 233–243.
- [56] M.K. Reagan, J.D. Morris, E.A. Herrstrom, M.T. Murrell, Uranium series and beryllium isotopic evidence for an extended history of subduction modification of the mantle below Nicaragua, *Geochim. Cosmochim. Acta* 58 (1994) 4199–4212.
- [57] R.S. Harmon, B.A. Barreiro, S. Moorbath, J. Hoefs, P.W. Francis, R.S. Thorpe, B. Deruelle, J. McHugh, J.A. Viglino, Reginal O-, Sr-, and Pb-isotope relationships in Late Cenozoic calc-alkaline lavas of the Andean Cordillera, *J. Geol. Sci. Lond.* 141 (1984) 803–822.
- [58] R. Barragan, D. Geist, M. Hall, P. Larson, M. Kurz, Subduction controls on the compositions of lavas from the Ecuadorian Andes, *Earth Planet. Sci. Lett.* 154 (1998) 153–166.
- [59] C. Annen, R.S.J. Sparks, Effects of repetitive emplacement of basaltic intrusions on thermal evolution and melt generation in the crust, *Earth Planet. Sci. Lett.* 203 (2002) 937–955.
- [60] N. Petford, K. Gallagher, Partial melting of mafic (amphibolitic) lower crust by periodic influx of basaltic magma, *Earth Planet. Sci. Lett.* 59 (2001) 1–17.
- [61] H.E. Huppert, R.S.J. Sparks, The generation of granitic magmas by intrusion of basalt into continental crust, *J. Petrol.* 29 (1988) 599–624.
- [62] N. Laube, J. Springer, Crustal melting by ponding of mafic magmas: a numerical model, *J. Volcanol. Geotherm. Res.* 81 (1988) 19–35.
- [63] J. Blundy, B. Wood, Mineral–melt partitioning of uranium, thorium and their daughters: reviews, in: Bourdon, Henderson, Lundstrom, Turner (Eds.), *Uranium-Series Geochemistry*, vol. 52, 2003, pp. 59–123.

- [64] A. Ewart, W.L. Griffin, Application of proton-microprobe data to trace-element partitioning in volcanic rocks, trace-element partitioning with application to magmatic processes, *Chem. Geol.* 117 (1994) 251–284.
- [65] S.F. Foley, M.G. Barth, G.A. Jenner, Rutile/melt partition coefficients for trace elements and an assessment of the influence of rutile on the trace element characteristics of subduction zone magmas, *Geochim. Cosmochim. Acta* 64 (2000) 933–938.
- [66] A.J. Irving, F.A. Frey, Distribution of trace elements between garnet megacrysts and host volcanic liquids of kimberlitic to rhyolitic composition, *Geochim. Cosmochim. Acta* 42 (1978) 771–787.
- [67] K. Cooper, M. Reid, Re-examination of crystal ages in recent Mount St. Helens lavas: implications for magma reservoir processes, *Earth Planet. Sci. Lett.* 213 (2003) 149–167.
- [68] J. Vazquez, M. Reid, Probing the accumulation history of the voluminous Toba magma, *Science* 305 (2004) 1991–1994.
- [69] Simon Turner, Rhiannon George, Dougal, A. Jerram, Neil Carpenter, Chris Hawkesworth, Case studies of plagioclase growth and residence times in island arc lavas from Tonga and the Lesser Antilles, and a model to reconcile discordant age information, *Earth Planet. Sci. Lett.* 214 (2003) 279–294.
- [70] J.M. Eiler, K.A. Farley, J.W. Valley, E.H. Hauri, C. Harmon, S.R. Hart, E.M. Stolper, Oxygen isotope variations in ocean island basalt phenocrysts, *Geochim. Cosmochim. Acta* 61 (1997) 2281–2293.
- [71] E. Heath, S.P. Turner, R. Macdonald, C.J. Hawkesworth, P. van Calsteren, Long magma residence times at an island arc volcano (Soufriere, St. Vincent) in the Lesser Antilles: evidence from  $^{238}\text{U}$ – $^{230}\text{Th}$  isochron dating, *Earth Planet. Sci. Lett.* 160 (1998) 49–63.
- [72] S. Turner, P. Evans, C. Hawkesworth, Ultrafast source-to-surface movement of melt at island arcs from  $^{226}\text{Ra}$ – $^{230}\text{Th}$  systematics, *Science* 292 (2001) 1363–1366.
- [73] M.D. Feineman, D.J. DePaolo, Steady-state  $^{226}\text{Ra}/^{230}\text{Th}$  disequilibrium in mantle minerals: implications for melt transport rates in island arcs, *Earth Planet. Sci. Lett.* 215 (2003) 339–355.
- [74] R.W. Le Maitre, P. Bateman, A. Dudek, J. Keller, M.J. Lameyre Le Bas, P.A. Sabine, R. Schmidt, H. Sorenson, A. Streckeisen, A. R. Woolley, B. Zanettin, *A Classification of Igneous Rocks and Glossary of Terms*, Blackwell, Oxford, 1989.
- [75] S.S. Sun, McDonough, Chemical and isotopic systematics of oceanic basalts: implications for mantle composition and processes, *Geol. Soc. Lond. Spec. Pub.* 42 (1989) 313–345.
- [76] T. Feininger, Eclogite and related high-pressure regional metamorphic rocks from the Andes of Ecuador, *J. Petrol.* 21 (1980) 107–140.